
Diffusion in Diffusion: Cyclic One-Way Diffusion for Text-Vision-Conditioned Generation

Yongqi Yang*
School of Computer Science
Wuhan University
yongqiyang@whu.edu.cn

Ruoyu Wang*
School of Computer Science
Wuhan University
wangruoyu@whu.edu.cn

Zhihao Qian
School of Computer Science
Wuhan University
qianzhihao@whu.edu.cn

Ye Zhu
Princeton University
yzhu96@hawk.iit.edu

Yu Wu
School of Computer Science
Wuhan University
wuyucs@whu.edu.cn

Abstract

Text-to-Image (T2I) generation with diffusion models allows users to control the semantic content in the synthesized images given text conditions. As a further step toward a more customized image creation application, we introduce a new multi-modality generation setting that synthesizes images based on not only the semantic-level textual input, but also on the pixel-level visual conditions. Existing literature first converts the given visual information to semantic-level representation by connecting it to languages, and then incorporates it into the original denoising process. Seemingly intuitive, such methodological design loses the pixel values during the semantic transition, thus failing to fulfill the task scenario where the preservation of low-level vision is desired (*e.g.*, ID of a given face image). To this end, we propose *Cyclic One-Way Diffusion* (COW), a training-free framework for creating customized images with respect to semantic-text and pixel-visual conditioning. Notably, we observe that sub-regions of an image impose mutual interference, just like physical diffusion, to achieve ultimate harmony along the denoising trajectory. Thus we propose to repetitively utilize the given visual condition in a cyclic way, by planting the visual condition as a high-concentration “seed” at the initialization step of the denoising process, and “diffuse” it into a harmonious picture by controlling a one-way information flow from the visual condition. We repeat the destroy-and-construct process multiple times to gradually but steadily impose the internal diffusion process within the image. Experiments on the challenging one-shot face and text-conditioned image synthesis task demonstrate our superiority in terms of speed, image quality, and conditional fidelity compared to learning-based text-vision conditional methods.

1 Introduction

Text-to-image (T2I) diffusion models, such as LDM [27], Imagen [30], DALL-E 2 [24], GLIDE [22], and CDCD [43], have made significant progress in generating high-quality images based on text prompts, which allow users to create semantically consistent images via textual descriptions. To further improve user controllability, recent works [29, 1, 5] seek to incorporate additional visual conditioning into the T2I models, extending the model input from pure text to multiple text-vision

¹These authors contributed equally to this work



Figure 1: Comparison with existing methods for Text-Vision to Image (TV2I) Generation. Given a particular face image and a text prompt, our approach can synthesize the given face in new contexts with higher fidelity, while existing methods only incorporate the semantic-level visual condition at most and thus fail to preserve pixel-level information such as facial identity and expression.

modalities. However, existing literature conditioned on text-vision input first extracts the semantic information of given visual images (usually in a few-shot manner) via pre-trained vision-language models [27, 24], and then integrates the processed semantic visual representations into the T2I base model in the form of additional textual conditioning. Despite their abilities to capture the high-level semantics of extra visual conditioning, the transition process from raw images to language-bridged semantics loses low-level visual information in pixels as illustrated in Fig. 1, thus failing to fulfill the application scenario where the preservation of low-level pixels is desired in the final synthesized images (*e.g.*, ID of a given face image). To this end, given a pre-trained T2I diffusion model, we introduce a novel multimodal generation task setting to synthesize images that well corresponds to the semantic-Text and pixel-Vision conditioning (TV2I), which allows users to create more customized images. Specifically, given a sentence and a single face image, we aim to generate an image that preserves the ID and expression of the face image conditioning and simultaneously matches the textual description.

While seeming intuitive, the preservation of low-level pixel information via a pre-trained T2I diffusion model is much more challenging than its counterpart with text-only conditioning. From the perspective of conditional generation, our proposed TV2I task is a generalization to [29, 5, 7, 1]. In other words, a well-preserved pixel-vision conditioning ensures the semantic consistency between the given visual input and the final synthesized image, however, the inverse correspondence does not hold in most cases (see examples in Fig. 1 from comparing methods). From another perspective of diffusion model understanding, the objective of our TV2I task limits the randomness of the model on the implanted visual region, which imposes additional restrictions on the stochastic denoising process. Specifically, the diffusion model benefits from the stochasticity in the random walk trajectory of the Markov process to ensure image quality during denoising [32, 42]. In other words, we risk impairing the generative ability of the base model and the quality of synthesized images by bluntly implanting the visual conditioning in the synthesized image. The above two challenges urge us to better investigate and understand the low-level pixel information evolution in the denoising trajectory of DDPMs and sophisticatedly design the corresponding method to fulfill our proposed task objective.

Interestingly, we found that pixels within a single image impose mutual interference with each other along both the diffusion and denoising directions to achieve ultimate harmony. This resembles the actual physical diffusion phenomena in thermodynamics, where a black ink drop diffuses in clean water, and this internal diffusion is crucial to the formation of the final harmonious results. This mutual interference drives each pixel to exchange information with the rest pixels, allowing us to effectively propagate information from the visual conditions throughout denoising, ensuring that the resulting images are fully integrated and fused with the desired visual condition.

By leveraging these properties and insights from the above key observation, we propose a novel training-free Cyclic One-Way Diffusion (COW) built upon a pre-trained T2I model to incorporate

given visual information. We propose to place a visual condition “seed” into the unimodal initialization space of the image (T -step) and impose the internal “diffusion” among pixels by repeatedly going through a particular phase among the original denoising process. To be specific, we first inverse the visual condition back to every diffusion step $\epsilon_{\{1:T\}}$ space by solving Ordinary Differential Equations (ODE) via Euler integration following DDIMs [32]. In addition, we introduce Seed Initialization to pre-define the high-level semantic layout of the synthesized image. We put and merge the input visual token at a random location on a pure gray image, and then inverse it back to the T space. After that, we start the denoising process and introduce the Cyclic One-Way process to repeatedly exploit a forced one-way diffusion from the visual condition to the other region. Extensive experiments show our method achieves results superior compared to state-of-the-art synthesis methods in terms of both condition correspondence and generation speed, without the need for any additional training.

2 Related Work

2.1 Text-to-Image (T2I) Model

Text-conditional image synthesis is a rapidly growing research area that aims to generate realistic and diverse images based on natural language descriptions. Early approaches mainly relied on GAN-based architectures [26, 38, 3, 39, 37, 18, 35, 13, 17, 14] to solve this problem. In recent years, Diffusion probabilistic models (DPMs) [9, 32, 2, 23, 33, 11, 36] have gradually become one of the most active and mainstream methods for vision generation tasks due to their impressive results and ability to support cross-modal synthesis mainly based on classifier-free conditional generation [10]. T2I models acquire their conditional generation ability generally by predicting added noise at a certain step with the additional text prompt during training. Diffusion-based text-to-image generation methods [27, 22, 30, 24, 25, 8] have achieved state-of-the-art results and become a primary choice of backbone for a multimodal conditional generation. Nevertheless, the current text-to-image generation models struggle to synthesize a highly customized image as the limited capability of text description.

2.2 Visual Condition based on T2I Model

Methods in this category require training a new diffusion model that accepts the visual condition as an additional input or introducing a new identifier for a given visual concept through fine-tuning pre-trained T2I models or converting the visual condition into text embedding space (prompt-tuning).

Fine-tuning. This branch of methods [29, 41, 12, 21, 15] usually fine-tune pre-trained T2I models. For example, ControlNet [41] extends the pre-trained large diffusion model with a trainable copy branch to support additional visual input conditions. Similar to ControlNet, the T2I-Adapter [21] differs mainly in the “learnable branch” network structure and other details. A recent novel approach, DreamBooth [29], binds the visual concept to a special ‘Rare-token Identifier’ and synthesizes images by implanting unique identifiers in prompts when inferencing. However, the models mentioned above all require some degree of fine-tuning, which are relatively costly in terms of time and computational resources. Additionally, DreamBooth [29] uses a small number of reference images to optimize a large number of parameters may lead to collapse and over-fitting.

Prompt-tuning. These works [5, 20, 7, 4] are probably the most relevant to our task. They also introduced a new pseudo-word to learn visual conditions in text embedding space. Specifically, this is a type of prompt-tuning distinct from fine-tuning, as the pre-trained models are frozen while the embedding of new pseudo-words is learnable. Also, there are works that introduce methods to add regular to learn a better text embedding [5], These methods can be understood as mapping visual conditions to pseudo-word embeddings, they can achieve style migration [7] and preserve higher-level semantic concepts. However, they also have obvious drawbacks, due to the text and visual conditions being in two distinct modalities, and unlike high semantic level guidance such as textual conditions, visual conditions such as detailed expression of the face can be a kind of complex low-level condition. So encoding visual conditions into a unified text space may cause unacceptable information loss in specific scenarios requiring more low-level semantics.

3 Method

We first introduce the preliminaries of related concepts of diffusion models in Sec. 3.1 and the newly discovered mutual influence of the denoising process in Sec. 3.2 and then present our Cyclic One-Way Diffusion (COW) procedure to repeatedly exploit a forced one-way diffusion from visual condition to other regions under the guidance of text condition.

3.1 Preliminaries

Diffusion Probabilistic Models. Denoising Diffusion Probabilistic Models (DDPMs [9]) introduce a Gaussian kernel to add noise to a data sample x_0 following:

$$q(x_t|x_{t-1}) = N(\sqrt{1 - \beta_t}x_{t-1}, \beta_t I), \quad (1)$$

where t represents diffusion step, $\{\beta_t\}_t^T$ are usually scheduled variance, and N represents Gaussian distribution. This can be further reformulated as,

$$x_t = \sqrt{\alpha_t/\alpha_{t-k}} \cdot x_{t-k} + \sqrt{1 - \alpha_t/\alpha_{t-k}} \cdot \epsilon, \quad (2)$$

where $\alpha_t = \prod_{i=0}^t (1 - \beta_i)$, and ϵ represents standard random Gaussian noise. Thus we can inject the corresponding diffusion step level of noise into any x_t to degenerate it back to x_{t-k} .

Denoising Diffusion Implicit Models. DDIM [32] has shown DDPM [9] can be reformulated as,

$$x_{t-1} = \underbrace{\sqrt{\alpha_{t-1}} \left(\frac{x_t - \sqrt{1 - \alpha_t} \epsilon_\theta^t(x_t)}{\sqrt{\alpha_t}} \right)}_{\text{“predicted } x_0\text{”}} + \underbrace{\sqrt{1 - \alpha_{t-1} - \sigma_t^2} \epsilon_\theta^t(x_t)}_{\text{“direction pointing to } x_t\text{”}} + \underbrace{\sigma_t \epsilon}_{\text{random noise}}, \quad (3)$$

where ϵ_θ is the implemented model (usually U-net [28]), and,

$$\sigma_t = \eta \sqrt{(1 - \alpha_{t-1}) / (1 - \alpha_t)} \sqrt{1 - \alpha_t / \alpha_{t-1}}, \quad (4)$$

as the factor controlling randomness during denoising. By setting $\eta = 0$, this can be written in an ODE form:

$$d\bar{x}(t) = \epsilon^{(t)} \left(\frac{\bar{x}(t)}{\sqrt{\sigma^2 + 1}} \right) d\sigma(t). \quad (5)$$

Solving the above equation using Euler integration, it can be further rewritten as:

$$x_t = \sqrt{\alpha_t} \left(\frac{x_{t-1}}{\sqrt{\alpha_{t-1}}} + \epsilon^{(t-1)}(x_{t-1}) \left(\sqrt{\frac{1 - \alpha_t}{\alpha_t}} - \sqrt{\frac{1 - \alpha_{t-1}}{\alpha_{t-1}}} \right) \right). \quad (6)$$

Thus we can not only get a deterministic denoising process, but most importantly, we can inverse the real image x_0 (visual condition) to x_t in any corresponding raw latent space ϵ_t [42] and reconstruct it back to x_0 almost perfectly. This motivates us to incorporate the visual condition at any denoising step by inverting and preserving most of the information.

Latent Diffusion Models (LDM). Different from Diffusion Probabilistic Models (DPMs) that perform denoising operations in the pixel space, the LDM-based [27] model performs the diffusion process in the latent space of an auto-encoder [6] to generate high-quality results at a faster speed and turn DPMs into more flexible conditional image generators by augmenting DPMs’ UNet backbone [28] with the cross-attention mechanism [34].

3.2 Properties of Denoising Process

We first design a qualitative experiment on Celeba64 pre-trained model to explore the internal diffusion phenomenon within the image during the denoising process, then try a quantitative experiment on LDM [27] to explore properties exhibited during the denoising process.

Internal Diffusion Phenomenon. To illustrate the internal diffusion within the image during the diffusion denoise process, we combine two known regions at different steps into one image and

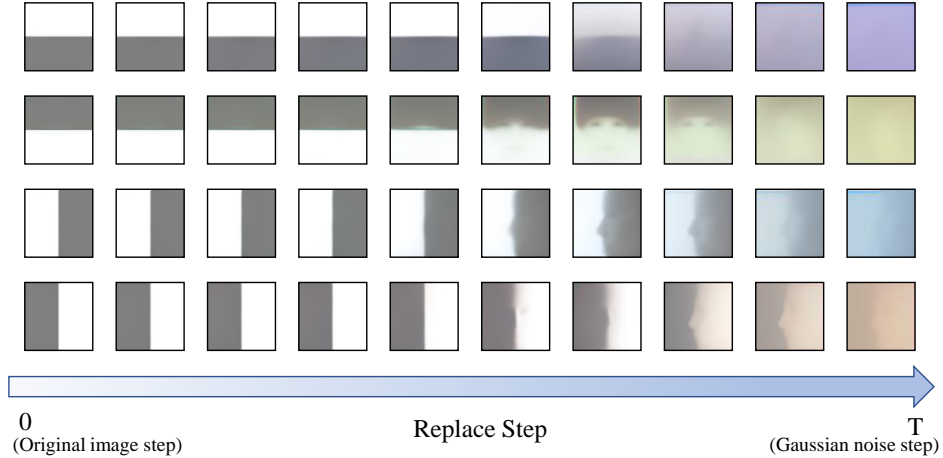


Figure 2: Illustration of the “spatial diffusion” within an image along the denoising process. We inverse pictures of pure gray and white back to x_t , merge them together with different layouts and then regenerate them back to x_0 via deterministic denoising. Different columns indicate different replacement steps t . The resulting images show how regions within an image diffuse into each other during denoising.

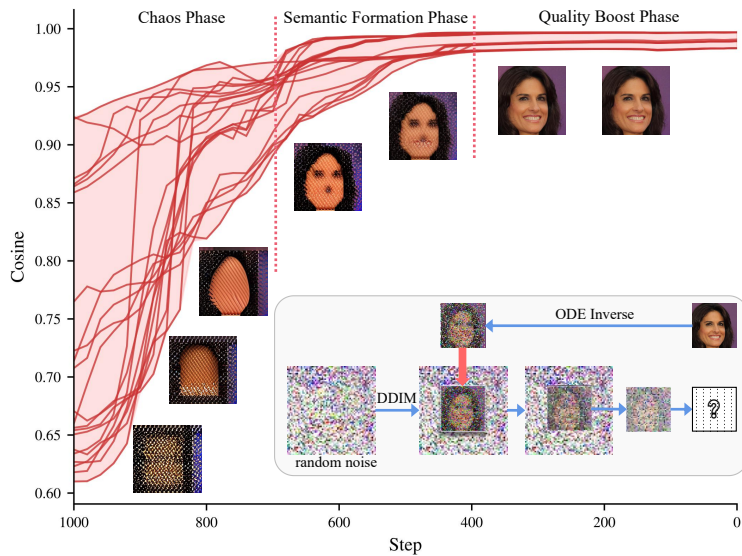


Figure 3: Illustration of the semantic formation process and the mutual interference. Each red curve represents a face disturb-and-reconstruct process. We only show one face for instance. We disturb the reconstruction process by sticking the origin image to random noise background at different steps. The cosine similarity between the original image and the reconstructed image increases as the denoising step goes.

regenerate it. Here we use Celeba64 pre-trained DDIM [32] model, inverse pictures of pure white and pure gray by solving ODE to obtain their intermediate steps. And then merge two half intermediate images into one using different layouts (*e.g.*, top, bottom, left, and right). As shown in Fig. 2, different color regions (gray and white) integrate with each other, which means there is a diffusion phenomenon between regions during the denoising process. The diffusion between regions becomes stronger as the replace step goes from 0 to T. Different position combinations lead to different diffusion results. Interestingly, the diffused area between gray and white can sometimes form a blurry face, which we assume comes from the tendency of the face model to converge to human faces.

Properties of Denoising Process. To assess the influence between regions during the denoising process, we inverse an image x_0 to obtain different transformed x_t , and plant it in a replacement

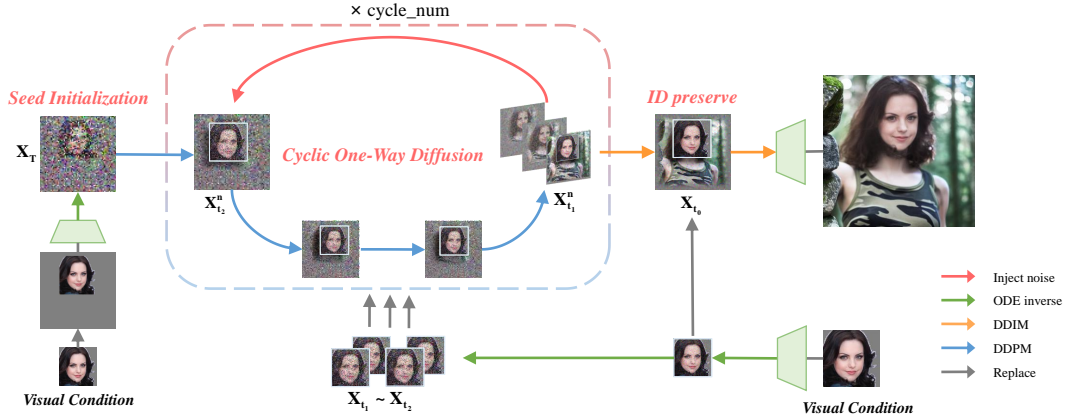


Figure 4: The pipeline of our proposed COW method. Given the input visual condition, we stick it on a predefined background and inverse it as the seed initialization of the denoising starting point. In the Cyclic One-Way Diffusion process, we “destroy” and “construct” the image in a cyclic way and ensure a one-way diffusion by consistently replacing it with corresponding x_t . See details in Sec. 3.3.

manner into a sub-region sampled by random Gaussian noise in the same step. We subsequently subject this composite noise map to several denoising steps before extracting the planted image to continue the generation process. As shown in Fig. 3, the influence level weakens with the denoising process. We found a similar phenomenon on text conditions, more results can be found in supplementary files.

In summary, we empirically partition the denoising process into three distinct phases, which characterize different evolution properties of pixel-level visions along the trajectory. The first phase, *i.e.*, the Chaos phase, is sensitive to text conditions and exhibits the foundation of high-level semantics (*e.g.*, the layout). However, a high degree of mutual influence makes it hard to be manually controlled. The second phase, *i.e.*, the Semantic Formation phase, strikes a balance between controllable mutual influence and the ability to respond to conditions. Finally, the Quality Boosting phase preserves most semantic information while adding more details such as textures to the generated image [42].

3.3 Training-free Cyclic One-way Diffusion

In this subsection, we illustrate how to take advantage of the properties of the three denoising phases to enable pixel-level visual conditioning preservation. Our approach involves three main components: Seed Initialization, Cyclic One-way Diffusion, and ID Preservation, as shown in Fig. 4.

Seed Initialization. It is common to bring the thread end close to the needle before threading. Using random initialization sampled from the Gaussian distribution may introduce high-level semantic conflicts between visual conditions and initial content (such as location). We propose to stick the visual condition on a user-specified place of a predefined background (usually gray), and inverse it from x_0 to x_T as the start point of the denoising process, which roughly preconditions more suitable high-level semantic information (such as the layout of contents) to effectively lower the difficulty of merging background and visual condition. Practically, Seed Initialization improves the quality of results, and greatly decreases the probability for results to fall into a bad local optimum.

Cyclic One-Way Diffusion (COW). Our primary goal is to generate a harmonious image grown from the visual conditions but keep the condition part unchanged. Seed Initialization could only generate a rough layout for better denoising starting point. To maintain the details of the visual condition, we need to consistently underline the visual information during the denoising process. Thus we need to maximize the diffusion process from the visual condition to the whole image while minimizing the other diffusion flow from the background to the visual condition. To achieve this, we propose Cyclic One-Way Diffusion to force internal mutual diffusion to be one-way diffusion, and continuously, repeatedly “destroy” and “construct” other sub-regions in a cyclic way.

To be specific, injecting the corresponding level of random Gaussian noise into x_{t-k} (begin of the cycle) could bring it back to t -th diffusion step. We thus could disturb the formed semantic information and create space for another round of “construct”. During denoising from x_t to x_{t-k} , we repeatedly replace the region of the visual condition using ODE inversed one in the corresponding step to achieve a one-way diffusion from the visual condition. Combining these processes, we complete a cycle of “destroy” and “construct”.

To implement COW, we selected two steps x_{t_1}, x_{t_2} in the Semantic Formation Phase as two ends of the cycle to attain controllable results. We empirically conclude that an optimal cycle length should be determined based on the shortest distance that guarantees effective diffusion from the visual condition to other sub-regions while providing sufficient space for the model to correct any inconsistencies or dissonance. The Cyclic One-Way Diffusion benefits the model from a one-way diffusion from the visual condition, creates additional play space by cycles of “destroy” and “construct”, and finally brings the background in harmony with the visual condition.

ID Preservation. The Semantic Formation phase is subject to some extent of uncertainty, thus the area of the visual condition in the generated image may be disturbed to some extent. Although this can improve the merging of the junction of the visual condition and the background, too much change can reduce the fidelity of the visual condition. To address this issue, we further impose the visual condition at an additional step x_{t_0} and replace the corresponding pixels at the early stage of the Quality Boosting Phase, similar to the process used in the Cyclic One-way Diffusion method. This approach can effectively preserve fidelity to the visual condition while still achieving a harmonious result.

4 Experiments

4.1 Experimental Setup

Benchmark. To simulate the visual condition processing in real scenarios, we adopt face image masks from CelebAMask-HQ [16] as our visual condition. For the text condition, we randomly select 100 textual descriptions from the MS COCO [19] captions that describe scenes of real images. Then we combine them together as the dual conditions for our TV2I task, with each text description corresponding to 3 random face images. We further remove contradiction pairs of text and visual conditions, such as “child” in the text but a face image of an old person). In order to make the text more consistent with the visual condition, we add “an upper half-body photo of” in front of each text condition during the image generation process.

Implementation Details. We implement our method and baselines on pre-trained T2I Stable Diffusion model [27] sd-v1-4, with default configuration condition scale set 7.5, noise level η set 1, image size set 512, and 50 steps generation. During generation, we set the visual condition size to 256 and randomly choose a place above half of the image to add the visual condition. We choose x_{t_1} to be step 25, x_{t_2} to be 35, x_{t_0} to be 20, cycle number to be 60. We perform all comparisons with baselines on 300 images and 100 texts (each text corresponding to 3 face images). We use one NVIDIA 4090 GPU to run experiments since the proposed model is training-free.

4.2 Comparison with State-of-the-Art Methods

We perform a comparison on current SOTA works incorporating the visual condition into pre-trained T2I models: DreamBooth [29] based on the code¹, TI [7], and UGM [1]. *DreamBooth* [29] introduces a rare-token identifier along with a class-prior for a more specific few-shot visual concept by finetuning pre-trained T2I model to obtain the ability to generate specific objects in results. *TI* [7] proposes to convert visual concept to word embedding space by training a new word embedding using a given visual condition and using it directly in the generation of results. *UGM* [1] introduce a universal guidance algorithm to enable binary guidance from arbitrary modalities to pre-trained diffusion models. They achieve visual guidance by utilizing extra classifier signals or face recognition models.

To evaluate the quality of the generated results for this new task, we consider two aspects, visual fidelity, and text fidelity. We follow the same evaluation metrics as in previous works [7, 29, 5],

¹<https://github.com/ShivamShrirao/diffusers/tree/main/examples/dreambooth>

Table 1: Quantitative analysis of our method compared with existing methods on conditional fidelity. Clip-Image, ID-Distance, and Face detection rate reflect the fidelity of the visual condition, while Clip-Text shows the fidelity to the textual condition. Our method outperforms others in all metrics.

Methodology	Clip-Image \uparrow	Clip-Text \uparrow	ID-Distance \downarrow	Face detection rate \uparrow	Time cost \downarrow
TI [7]	0.538	0.206	1.257	62.33%	2008s
DreamBooth [29]	0.477	0.210	1.244	73.33%	450s
UGM [1]	0.409	0.206	1.407	45.66%	75s
COW (ours)	0.604	0.215	0.651	99.00%	65s

Table 2: Evaluation results of the human study including two criteria, condition consistency, and general fidelity. We achieve superior condition consistency, but at a cost of some loss in general fidelity, since the other methods neglect the visual condition and lead to a more flexible and in-domain generation.

Methods	Condition Consistency	General Fidelity
TI [7]	04.22%	06.56%
DreamBooth [29]	10.11%	44.78%
UGM [1]	08.44%	28.33%
COW (ours)	77.22%	20.44%

namely the CLIP-space cosine-similarity. Additionally, since image similarity may not distinguish between different identities with highly similar semantics, we use the Face ID Distance and the face detection rate to assess the fidelity of the visual condition. Results are shown in Tab. 1.

CLIP-space Cosine-similarity. We use pretrained CLIP (ViT-B/32) to evaluate the fidelity of generated image to text and visual condition. We achieved 0.604 on Clip-Image, significantly exceeding other works in terms of fidelity to visual conditions, while preserving the fidelity to text conditions (Clip-Text similarity).

Face Detection Rate. We use multi-task cascaded convolutional networks (MTCNN) [40] as the face detection module to detect the presence and location of the face. Results show that our method almost perfectly retains faces (the given visual condition) in the synthesized images.

Face ID Distance. We use the face ID of the detected region (if not None) from generated images to compare the distance to the ID of the visual condition using facenet [31] as the face recognition module. Our results show a much better preservation of the ID of a given face.

These qualitative results prove that our method outperforms previous works in fidelity to visual and text conditions. From the Face detection rate and ID Distance, we can see that when applied to a limited number of complex visual conditions (human face), explicitly adding low-level visual pixels can force the model to generate high-fidelity results of the visual condition. In addition, our method is training-free, thus we can generate the prediction using fewer computations.

4.3 Tradeoffs between Text and Visual conditions

As shown in Fig. 5, our approach demonstrate the ability to trade off between visual and text conditions. For example, when given a photo of a *young* woman but the text is “an *old* person”, our method can make the woman older to meet the text description by adding wrinkles, changing skin elasticity and hair color, etc. while maintaining the identity information of the given woman. Besides, even if we diffuse the visual conditions via constant replacement, we can still obtain Van Gogh-style face and blurred face pictures guided by the text condition. This may benefit from the integration guided by text condition between visual condition and background during the denoising process after ID Preservation.

4.4 Human Evaluation

We further evaluate our method via human user feedback. We designed two base criteria and invited 30 volunteers to be involved in this human evaluation. The two criteria are: 1. **Condition correspondance**: whether the generated image better matches the visual and textual conditions; 2.

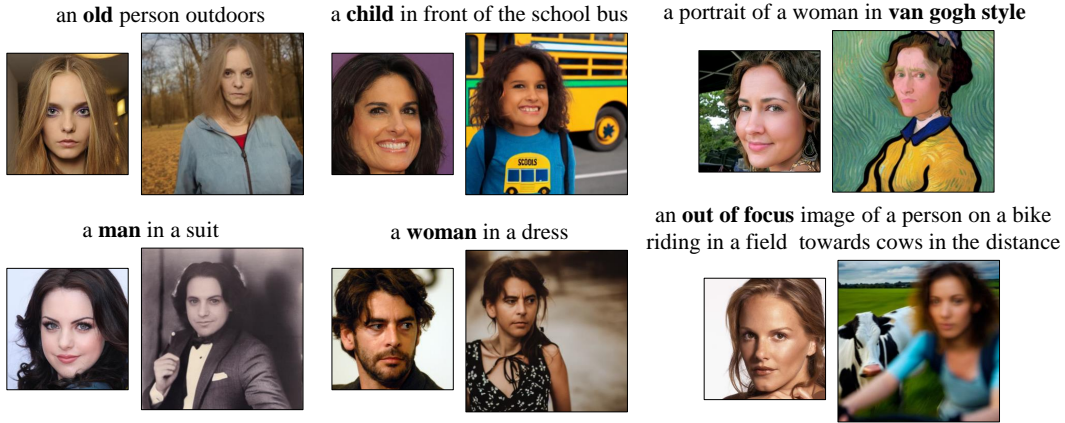


Figure 5: The adaptation of the visual condition to align with the text condition while maintaining the identity information of the visual condition. In each pair of images, the smaller image is the given visual condition and the other is the generated result. The bolded parts of the text conditions highlight the conflicts.

General fidelity: whether the chosen image looks more like a real image involving image richness, face naturalness, and overall image fidelity. Note that there are NO text and visual conditions present in the latter criterion to avoid the impact of conditions.

We ask volunteers to choose their most preferable image from shuffled images, including ours and the three compared methods. Each image is evaluated by both criteria and six different volunteers. Totally, we obtain 1,800 answers for 300 image groups evaluated, and we list these results in Tab. 2. We find that our method receives a significant performance (77.22% of the votes) in terms of condition correspondence compared to the three methods, where the second best one, DreamBooth [29] only gets 10.11% votes. The results strongly demonstrate that our method better satisfies the text and visual conditions while preserving target fidelity as much as possible. As the cost of meeting strict conditions, the votes on the general fidelity for our method is less than the compared works. We checked the results and believe the main reason is a considerable part of images generated by the three compared methods do not meet the visual conditions and show higher quality as they are actually generating in-domain samples. In addition, we also find users prefer to pick simple images (*e.g.*, a scene/object photo without any human, or a small human that is too blurred to be seen clearly) since people are more sensitive and picky with synthesized human images.

4.5 Ablation Studies

We analyze Seed Initialization and the cycle number to verify that placing “seed” in Chaos phase can provide a better starting point with high-level semantic predefined, and explain our proposed one-way cycle do help the “seed” diffuse into other regions of the background.

Different Initialization Position. We show the ablation analysis on Seed Initialization (SI) to see its effectiveness in Fig. 6. The first three columns show different initialization positions for SI, which simulate user customization of visual conditions. We can see our model can freely generate reasonable images given the pre-defined initialization position.

Different Seed Initialization Background. We also try white, black, and random noise backgrounds as the pre-defined background images for SI. The results show using these backgrounds could lightly decrease the quality of generated images compared to the ones in the gray (default) background. We argue this originates from the fact that the average color value (gray) is a better starting point for all possible synthesized images.

Ablation of Seed Initialization. The results w/o SI exhibit an unnatural merging between background and visual condition, as another person emerges separately from the visual condition. This clearly shows the effectiveness of our SI. Without SI, we can not pre-generate the image layout during the Chaos Phase, where the model only fits the textual condition without knowing the visual condition.

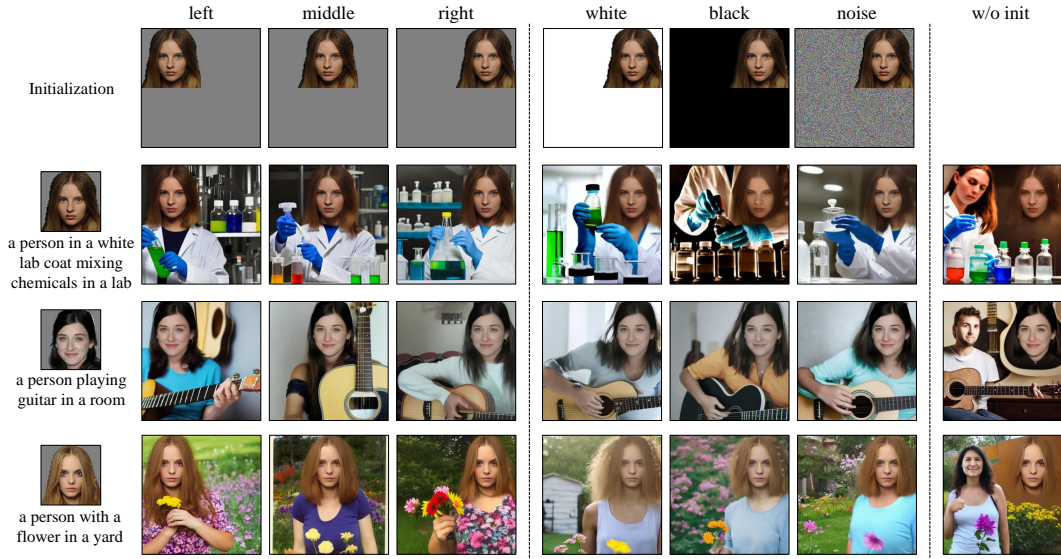


Figure 6: Ablation study on Seed Initialization. Given the left-most visual and text conditions, we show generated images at different initialization positions (left, middle, and right), with different initial backgrounds (gray, white, black, and random noise), and without Seed Initialization.

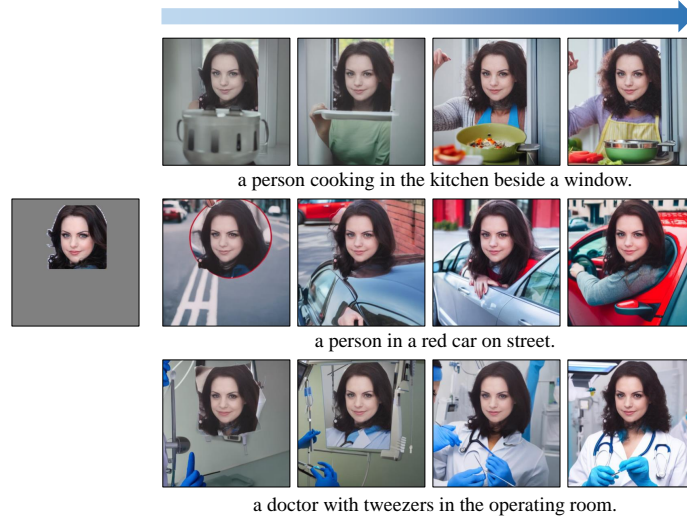


Figure 7: Analysis of the cycling process that diffuses “visual seed” to its surroundings. The leftmost figure shows a given face condition and its initialization position. The right shows the images generated given different text conditions. The cycle number increases from the left to the right.

For example, the model may already generate a person at other positions rather than the user’s pre-defined location, which is impossible for us to meet the strict visual condition restrictions given such a layout.

Analysis of Cyclic One-Way Diffusion. To demonstrate the effect of COW on the internal diffusion within the image, we conduct experiments with η set to 0 from T -th to t_1 -th step. As the cycle goes on, the background pixels gradually match the textual condition and fuse with the given visual face condition. The results are shown in Fig. 7. At the beginning of cycles, the visual condition face is isolated while the image is getting to fit the textual condition by forming more richer scenes. As the cycle goes on, we find the generated images show a clear procedure for growing a body from the given face condition. The background and visual condition are getting more and more harmonious as

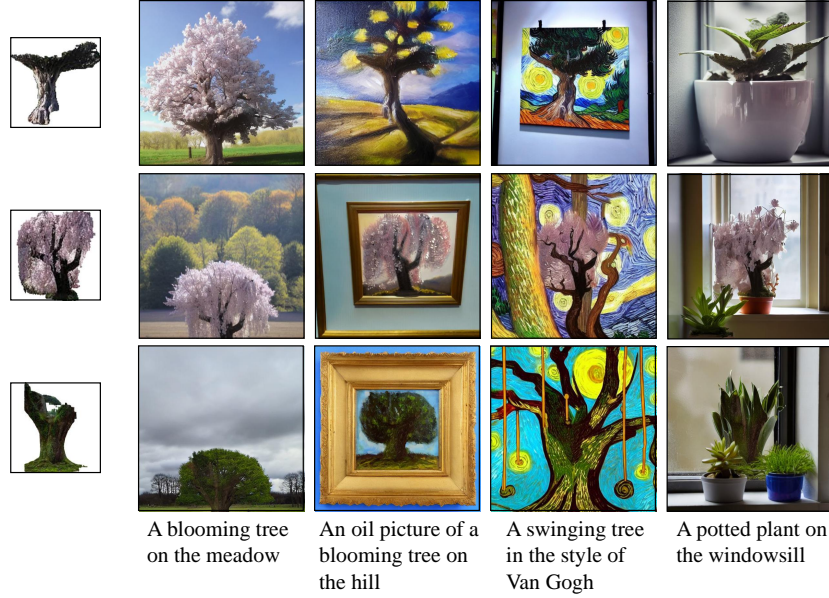


Figure 8: Generated results using *tree* as visual conditions with different text conditions. The leftmost column is the visual conditions and the bottom is the text conditions.

the completion of the human body. It vividly demonstrates that the information in the visual condition keeps spreading and diffusing to the surrounding region along with cycles. In addition, the model is capable of understanding the semantics of the implanted visual conditions properly.

4.6 Generalized Visual Condition

We directly apply our method to other visual conditions than the human face to show its scalability. As in Fig. 8 and Fig. 9, we show results of trees and cats with different text conditions. Our method harmoniously grows a whole body out of the visual condition under the guidance of the text condition. What’s more, our method has the ability to achieve style transfer results (such as “Van Gogh”, and “oil picture”) and transplant one class onto the other (*e.g.*, “trees” to “potted plant”), seeking a balance between preserving the visual condition and meeting given text condition.

5 Conclusion and Discussion

In this paper, we study a new generation setting that synthesizes images based on both semantic-text and pixel-visual conditions. Different from existing works that convert visual information to semantic language representations, we propose a training-free Cyclic One-Way diffusion framework, where we depart from a high-concentration visual “seed” at the initialization step and “diffuse” it into a harmonious picture via cycles of “destroy” and “construct”. Experiments demonstrate our method could generate images with high fidelity to both semantic-text and pixel-visual conditions in a training-free, lightweight, efficient, and effective manner.

Limitations. Although we benefit a lot from explicitly utilizing the visual condition and variable size of LDM input, these can bring limitations in some scenarios. The pre-trained diffusion model is not robust enough to handle strong conflicts between the visual and the text condition. For example, when given the text “a puppy at a person’s feet”, and a face condition at the lower part of the image, it is very hard to generate a harmonious result that both fits two conditions. In this case, the model would follow the guidance of the text generally.

Since LDM eliminates high-frequency details in the perceptual compression stage, and the reconstruction error of latent space will be enlarged accordingly, it is difficult to maintain the reconstruction ability for extremely small-size images.

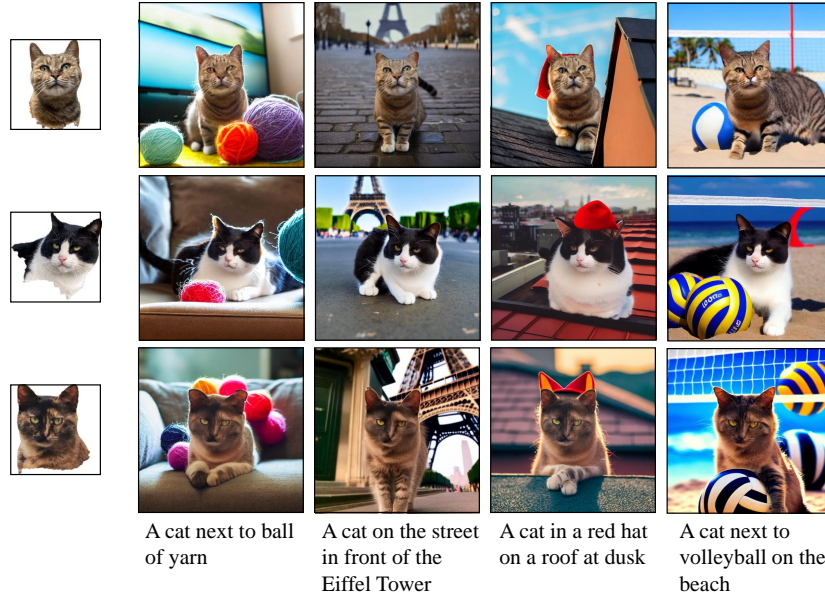


Figure 9: Generated results using *cats* as visual conditions with different text conditions. The leftmost column is the visual conditions and the bottom is the text conditions.

Social Impact. Image generation and image manipulation have been greatly used in art, entertainment, aesthetics, and other common use cases in people’s daily life. But it can be abused in telling lies for harassment, distortion, and other malicious behavior. Too much abuse of generated images will decrease the credibility of the image. Our work doesn’t surpass the capabilities of professional image editors, which adds to the ease of use of this proposed process. Since our model fully builds on the pre-trained T2I model, all the works distinguishing the authenticity of the image should be able to be directly applied to our results.

References

- [1] Arpit Bansal, Hong-Min Chu, Avi Schwarzschild, Soumyadip Sengupta, Micah Goldblum, Jonas Geiping, and Tom Goldstein. Universal guidance for diffusion models. *arXiv preprint arXiv:2302.07121*, 2023.
- [2] Prafulla Dhariwal and Alexander Nichol. Diffusion models beat gans on image synthesis. *NeurIPS*, 34:8780–8794, 2021.
- [3] Hao Dong, Simiao Yu, Chao Wu, and Yike Guo. Semantic image synthesis via adversarial learning. In *ICCV*, pages 5706–5714, 2017.
- [4] Wenkai Dong, Song Xue, Xiaoyue Duan, and Shumin Han. Prompt tuning inversion for text-driven image editing using diffusion models. *arXiv preprint arXiv:2305.04441*, 2023.
- [5] Ziyi Dong, Pengxu Wei, and Liang Lin. Dreamartist: Towards controllable one-shot text-to-image generation via contrastive prompt-tuning. *arXiv preprint arXiv:2211.11337*, 2022.
- [6] Patrick Esser, Robin Rombach, and Bjorn Ommer. Taming transformers for high-resolution image synthesis. In *CVPR*, pages 12873–12883, 2021.
- [7] Rinon Gal, Yuval Alaluf, Yuval Atzmon, Or Patashnik, Amit H Bermano, Gal Chechik, and Daniel Cohen-Or. An image is worth one word: Personalizing text-to-image generation using textual inversion. *arXiv preprint arXiv:2208.01618*, 2022.
- [8] Shuyang Gu, Dong Chen, Jianmin Bao, Fang Wen, Bo Zhang, Dongdong Chen, Lu Yuan, and Baining Guo. Vector quantized diffusion model for text-to-image synthesis. In *CVPR*, pages 10696–10706, 2022.
- [9] Jonathan Ho, Ajay Jain, and Pieter Abbeel. Denoising diffusion probabilistic models. *NeurIPS*, 33:6840–6851, 2020.
- [10] Jonathan Ho and Tim Salimans. Classifier-free diffusion guidance. *arXiv preprint arXiv:2207.12598*, 2022.
- [11] Emiel Hoogeboom, Alexey A Gritsenko, Jasmijn Bastings, Ben Poole, Rianne van den Berg, and Tim Salimans. Autoregressive diffusion models. *arXiv preprint arXiv:2110.02037*, 2021.
- [12] Lianghua Huang, Di Chen, Yu Liu, Yujun Shen, Deli Zhao, and Jingren Zhou. Composer: Creative and controllable image synthesis with composable conditions. *arXiv preprint arXiv:2302.09778*, 2023.
- [13] Tero Karras, Samuli Laine, and Timo Aila. A style-based generator architecture for generative adversarial networks. In *CVPR*, pages 4401–4410, 2019.
- [14] Tero Karras, Samuli Laine, Miika Aittala, Janne Hellsten, Jaakko Lehtinen, and Timo Aila. Analyzing and improving the image quality of stylegan. In *CVPR*, pages 8110–8119, 2020.
- [15] Nupur Kumari, Bingliang Zhang, Richard Zhang, Eli Shechtman, and Jun-Yan Zhu. Multi-concept customization of text-to-image diffusion. *arXiv preprint arXiv:2212.04488*, 2022.
- [16] Cheng-Han Lee, Ziwei Liu, Lingyun Wu, and Ping Luo. Maskgan: Towards diverse and interactive facial image manipulation. In *CVPR*, pages 5549–5558, 2020.
- [17] Wenbo Li, Pengchuan Zhang, Lei Zhang, Qiuyuan Huang, Xiaodong He, Siwei Lyu, and Jianfeng Gao. Object-driven text-to-image synthesis via adversarial training. In *CVPR*, pages 12174–12182, 2019.
- [18] Chen-Hsuan Lin, Ersin Yumer, Oliver Wang, Eli Shechtman, and Simon Lucey. ST-GAN: Spatial transformer generative adversarial networks for image compositing. In *CVPR*, pages 9455–9464, 2018.
- [19] Tsung-Yi Lin, Michael Maire, Serge Belongie, James Hays, Pietro Perona, Deva Ramanan, Piotr Dollár, and C Lawrence Zitnick. Microsoft coco: Common objects in context. In *ECCV*, pages 740–755. Springer, 2014.
- [20] Yiyang Ma, Huan Yang, Wenjing Wang, Jianlong Fu, and Jiaying Liu. Unified multi-modal latent diffusion for joint subject and text conditional image generation. *arXiv preprint arXiv:2303.09319*, 2023.
- [21] Chong Mou, Xintao Wang, Liangbin Xie, Jian Zhang, Zhongang Qi, Ying Shan, and Xiaohu Qie. T2i-adapter: Learning adapters to dig out more controllable ability for text-to-image diffusion models. *arXiv preprint arXiv:2302.08453*, 2023.
- [22] Alex Nichol, Prafulla Dhariwal, Aditya Ramesh, Pranav Shyam, Pamela Mishkin, Bob McGrew, Ilya Sutskever, and Mark Chen. Glide: Towards photorealistic image generation and editing with text-guided diffusion models. *arXiv preprint arXiv:2112.10741*, 2021.
- [23] Alexander Quinn Nichol and Prafulla Dhariwal. Improved denoising diffusion probabilistic models. In *ICML*, pages 8162–8171, 2021.
- [24] Aditya Ramesh, Prafulla Dhariwal, Alex Nichol, Casey Chu, and Mark Chen. Hierarchical text-conditional image generation with clip latents. *arXiv preprint arXiv:2204.06125*, 2022.
- [25] Aditya Ramesh, Mikhail Pavlov, Gabriel Goh, Scott Gray, Chelsea Voss, Alec Radford, Mark Chen, and Ilya Sutskever. Zero-shot text-to-image generation. In *ICML*, pages 8821–8831,

- 2021.
- [26] Scott Reed, Zeynep Akata, Xinchun Yan, Lajanugen Logeswaran, Bernt Schiele, and Honglak Lee. Generative adversarial text to image synthesis. In *ICML*, pages 1060–1069, 2016.
 - [27] Robin Rombach, Andreas Blattmann, Dominik Lorenz, Patrick Esser, and Björn Ommer. High-resolution image synthesis with latent diffusion models. In *CVPR*, pages 10684–10695, 2022.
 - [28] Olaf Ronneberger, Philipp Fischer, and Thomas Brox. U-net: Convolutional networks for biomedical image segmentation. In *Medical Image Computing and Computer-Assisted Intervention*, pages 234–241. Springer, 2015.
 - [29] Nataniel Ruiz, Yuanzhen Li, Varun Jampani, Yael Pritch, Michael Rubinstein, and Kfir Aberman. Dreambooth: Fine tuning text-to-image diffusion models for subject-driven generation. *arXiv preprint arXiv:2208.12242*, 2022.
 - [30] Chitwan Saharia, William Chan, Saurabh Saxena, Lala Li, Jay Whang, Emily L Denton, Kamyar Ghasemipour, Raphael Gontijo Lopes, Burcu Karagol Ayan, Tim Salimans, et al. Photorealistic text-to-image diffusion models with deep language understanding. *NeurIPS*, pages 36479–36494, 2022.
 - [31] Florian Schroff, Dmitry Kalenichenko, and James Philbin. Facenet: A unified embedding for face recognition and clustering. In *CVPR*, pages 815–823, 2015.
 - [32] Jiaming Song, Chenlin Meng, and Stefano Ermon. Denoising diffusion implicit models. *arXiv preprint arXiv:2010.02502*, 2020.
 - [33] Yang Song, Jascha Sohl-Dickstein, Diederik P Kingma, Abhishek Kumar, Stefano Ermon, and Ben Poole. Score-based generative modeling through stochastic differential equations. *arXiv preprint arXiv:2011.13456*, 2020.
 - [34] Ashish Vaswani, Noam Shazeer, Niki Parmar, Jakob Uszkoreit, Llion Jones, Aidan N Gomez, Łukasz Kaiser, and Illia Polosukhin. Attention is all you need. *NeurIPS*, 30, 2017.
 - [35] Huikai Wu, Shuai Zheng, Junge Zhang, and Kaiqi Huang. GP-GAN: Towards realistic high-resolution image blending. In *ACM MM*, pages 2487–2495, 2019.
 - [36] Jay Zhangjie Wu, Yixiao Ge, Xintao Wang, Weixian Lei, Yuchao Gu, Wynne Hsu, Ying Shan, Xiaohu Qie, and Mike Zheng Shou. Tune-a-video: One-shot tuning of image diffusion models for text-to-video generation. *arXiv preprint arXiv:2212.11565*, 2022.
 - [37] Tao Xu, Pengchuan Zhang, Qiuyuan Huang, Han Zhang, Zhe Gan, Xiaolei Huang, and Xiaodong He. AttnGAN: Fine-grained text to image generation with attentional generative adversarial networks. In *CVPR*, pages 1316–1324, 2018.
 - [38] Han Zhang, Tao Xu, Hongsheng Li, Shaoting Zhang, Xiaogang Wang, Xiaolei Huang, and Dimitris N Metaxas. StackGAN: Text to photo-realistic image synthesis with stacked generative adversarial networks. In *ICCV*, pages 5907–5915, 2017.
 - [39] Han Zhang, Tao Xu, Hongsheng Li, Shaoting Zhang, Xiaogang Wang, Xiaolei Huang, and Dimitris N Metaxas. StackGAN++: Realistic image synthesis with stacked generative adversarial networks. *TPAMI*, 41(8):1947–1962, 2018.
 - [40] Kaipeng Zhang, Zhanpeng Zhang, Zhifeng Li, and Yu Qiao. Joint face detection and alignment using multitask cascaded convolutional networks. *IEEE signal processing letters*, 23(10):1499–1503, 2016.
 - [41] Lvmin Zhang and Maneesh Agrawala. Adding conditional control to text-to-image diffusion models. *arXiv preprint arXiv:2302.05543*, 2023.
 - [42] Ye Zhu, Yu Wu, Zhiwei Deng, Olga Russakovsky, and Yan Yan. Boundary guided mixing trajectory for semantic control with diffusion models. *arXiv preprint arXiv:2302.08357*, 2023.
 - [43] Ye Zhu, Yu Wu, Kyle Olszewski, Jian Ren, Sergey Tulyakov, and Yan Yan. Discrete contrastive diffusion for cross-modal and conditional generation. *arXiv preprint arXiv:2206.07771*, 2022.

Appendices

In Appendix. A, we provide additional TV2I generation results involving results with different visual seed sizes, conflicts between visual and text conditions, and more results compared with the baseline. The human evaluation interface is in Appendix. B. We include a more detailed pipeline of our method in Appendix. C. We also illustrate varying sensitivity to text conditions of the denoising process in Appendix D and show the semantic formation process of different sizes in Appendix E.

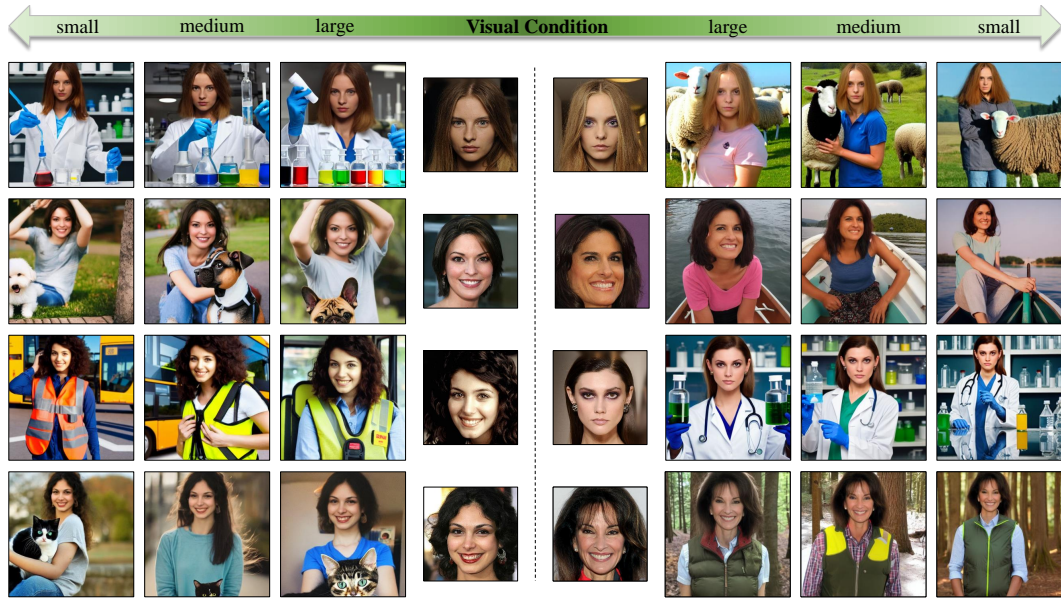


Figure 10: Generated results from different sizes of visual condition. We experimented with Seed Initialization for different sizes of large, medium, and small, respectively.



Figure 11: Several examples of the visual condition contradicting the text condition. The bolded parts of the text conditions highlight the conflicts.

A TV2I Generation Results Comparison and Analysis

A.1 Different Sizes of Visual Condition

We directly change the face size of the visual condition and pad it to 256×256 to apply in the original process. As shown in Fig. 10, our method still remains satisfactory results, although the smaller visual condition is more susceptible to the background.

A.2 Contradiction between Visual and Text Condition

Our approach demonstrates the ability to trade-off between visual and text conditions as in Fig. 5. However, when there is a great contradiction in the layout of the space required by visual and text conditions, it will be extremely difficult to generate images that satisfy both conditions in harmony. For example, when the text condition is “a person with his *back* to the camera”, it is impossible to insert the given front view of the face into the generated image.

A.3 More Image Comparisons with Baseline

In Fig. 12, we include a more intuitive comparison with baseline results. We compared current SOTA work that incorporates visual conditions into pre-trained T2I models: DreamBooth [29], TI [7], and UGM [1].

DreamBooth [29] binds specific few-shot visual concepts to a rare-token identifier along with a class-prior fine-tuning the pre-trained T2I model to gain the ability to produce a specific object in the result. TI [7] proposes to convert a visual concept into a word embedding space by training a new word embedding using a given visual condition and generating it by including it directly when inferencing. UGM [1] introduces a universal guidance algorithm to enable binary guidance from arbitrary modalities to pre-trained diffusion models. They achieve visual guidance by utilizing extra classifier signals or face recognition models. Completely different from these above methods, we propose a novel training-free framework by repeating the destroy-and-construct process multiple times to gradually but steadily impose the internal diffusion process within the image.

B Human Evaluation Details

We conduct a human evaluation based on two criteria: 1) **Condition correspondance**: whether generated image better matches both the visual and textual conditions; 2) **General fidelity**: whether the chosen image looks more like a real image involving image richness, face naturalness, and overall image fidelity. Note that no text and visual conditions are present in the latter criterion to avoid the impact of conditions. We show examples of questionnaire systems received by volunteers regarding these two criteria in Fig. 13 and Fig. 14.

C Cyclic One-Way Diffusion (COW) Details

In the Seed Initialization process, we stick the visual condition on a user-specified place of a predefined background (usually gray), and inverse it from x_0 to x_T as the start point of the denoising process, which roughly preconditions more suitable high-level semantic information (such as the layout of contents) to effectively lower the difficulty of merging background and visual condition. The initialized x_T goes through the stochastic denoising process of $eta = 1$ to x_{t_1} at the start of the cycle. In the Cyclic One-Way Diffusion process, we diffuse the x_{t_1} back to x_{t_2} by injecting the corresponding level of random Gaussian noise. And during denoising from x_{t_2} back to x_{t_1} , we repeatedly replace the region of the visual condition via inversed one in the corresponding step to achieve a one-way diffusion from the visual condition to other sub-regions. Thus we could disturb the formed semantic information and create adequate time and space for another round of “construct”, and diffuse the visual condition into a harmonious picture by controlling a one-way information flow from the visual condition. During the Quality Boosting Phase after the end of the cycle, we utilize the deterministic denoising of $eta = 0$ from x_{t_1} to x_{t_0} to better preserve the visual condition. Additionally, we impose the visual condition at step x_{t_0} , similar to the replacement used in the Cyclic One-way Diffusion. This approach can effectively preserve fidelity to visual conditions while still achieving a harmonious result. A more detailed version of the method pipeline is shown in Fig. 15.

D Sensitivity to Text Condition during Denoising

We study the model’s sensitivity to text conditions during the denoising process by injecting text conditions at different denoising steps. We replace a few unconditional denoising steps with text-conditioned ones during the generation of image random sampled from Gaussian noise. We calculate the Clip cosine similarity between the final generated image and text condition. As shown in Fig 16,

the model is more sensitive to text conditions in the early denoising stage and less sensitive in the late stage. This also demonstrates our method reasonably utilizes the sensitivity to text conditions through proposed Seed Initialization and Cyclic One-Way Diffusion.

E Illustration of Semantic Formation Process of Different Sizes

To see the degree of impact exerted on images of different sizes during the denoising process, we conduct the same experiments with images of two different sizes (128×128 , 256×256). We inverse images to x_t , and reconstruct them with disturbance introduced by sticking them to a random noise background (512×512) at the corresponding step for 100 steps. We calculate the MSE loss of the original image and the final reconstructed image after being disturbed. As shown in Fig 17, the semantic is settled earlier when the size is larger.

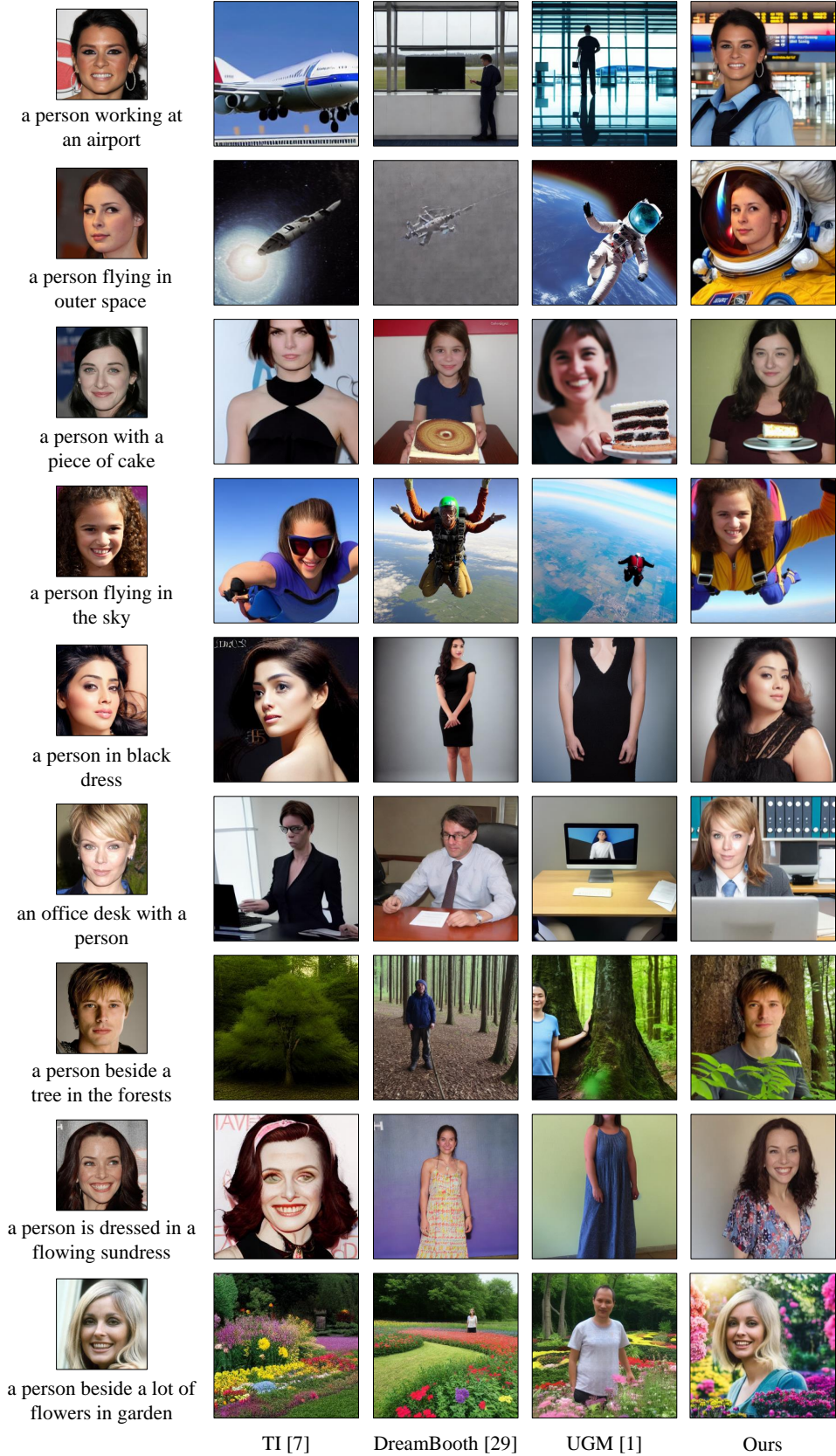


Figure 12: Comparison of our COW-generated images with TV2I baseline.

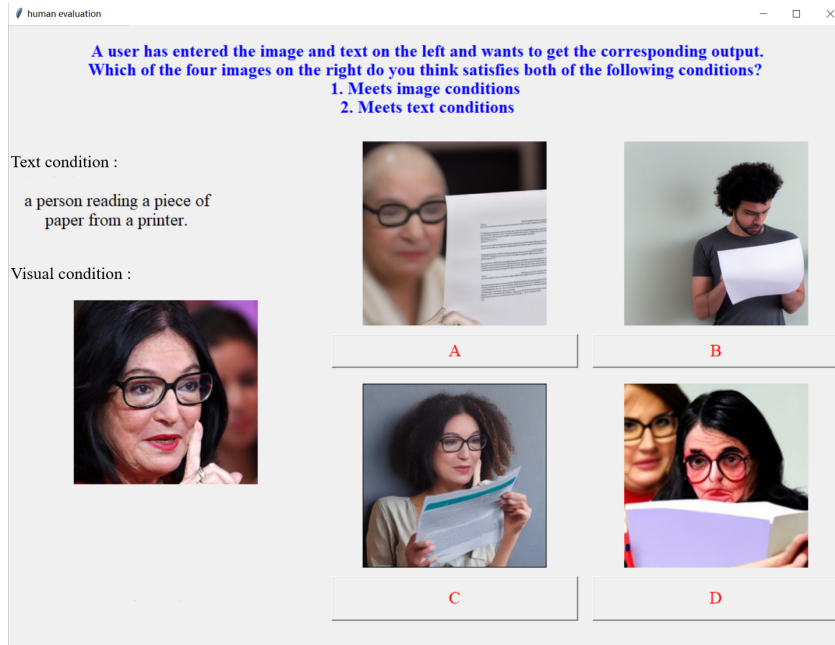


Figure 13: The interface of our human study on conditional consistency.



Figure 14: The interface of our human study on general fidelity.

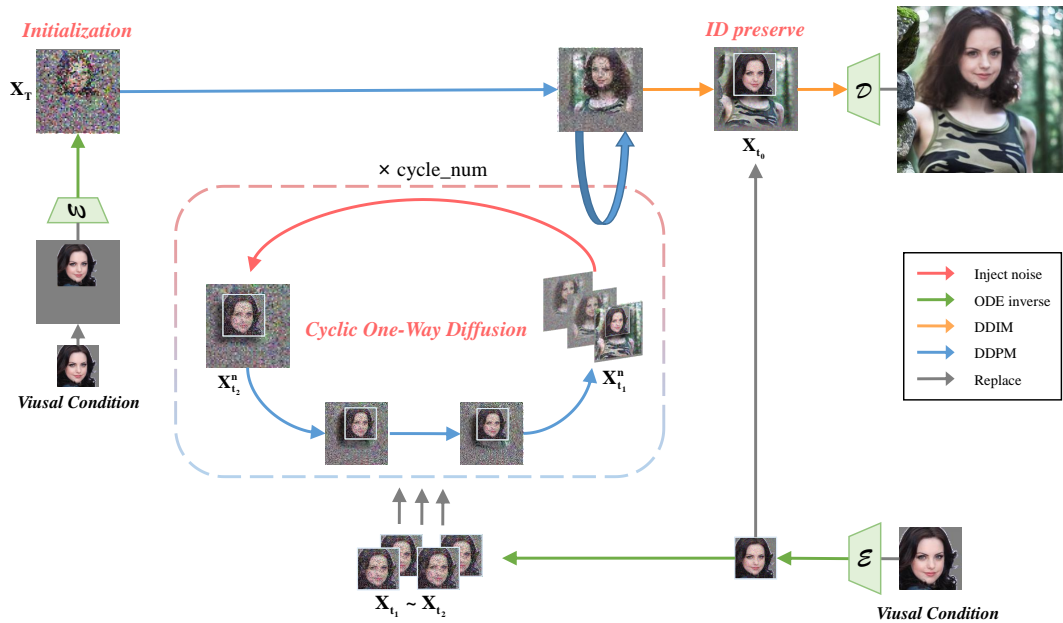


Figure 15: **The more detailed pipeline of our proposed COW method.** We have shown a simplified version in our main paper for better clarification. This is a more detailed version.

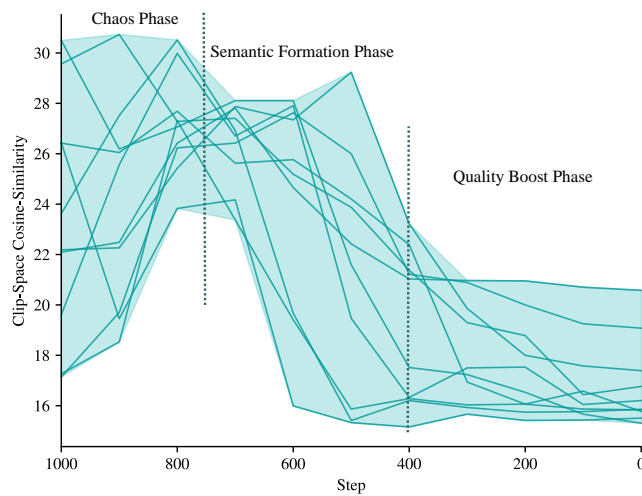


Figure 16: **Text-sensitivity during denoising process.** Each line represents a CLIP cosine similarity between generated image and text with the text condition injected at different steps. The image is generated in 1000 overall unconditional denoising process with 100 steps text conditional guidance starting from t . Generally, the denoising process is more responsive to the text condition in the beginning and almost stops reacting to the text condition when high-level semantics is settled.

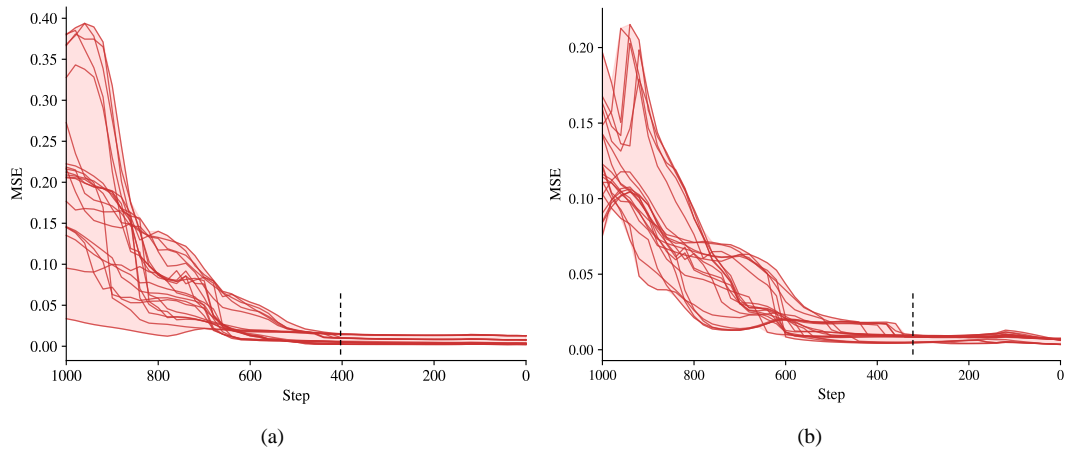


Figure 17: Different sizes come with different semantic formation processes. Each red curve represents a face disturb-and-reconstruct process, (a) size is 256×256 and (b) size is 128×128 . We disturb the reconstruction process by sticking the origin image to random noise background (512×512) at different steps. The general semantic is settled earlier when the size is larger.